IEEE Access
Multidisciplinary ⋮ Rapid Review ⋮ Open Access Journal

Received 9 July 2023, accepted 14 August 2023, date of publication 18 August 2023, date of current version 28 August 2023.

Digital Object Identifier 10.1109/ACCESS.2023.3306597

RESEARCH ARTICLE

Research on Adaptive Two-Point Energy Management Strategy and Optimization for Range-Extended Electric Vehicle

CHENG CHANG[1], ZIKAI FAN[2,3], ZHIHUI WANG[1], AND HANWU LIU[2,4]

[1]School of Vehicle and Traffic Engineering, Henan Institute of Technology, Xinxiang, Henan 453003, China
[2]State Key Laboratory of Automotive Simulation and Control, Jilin University, Changchun, Jilin 130022, China
[3]College of Automotive Engineering, Jilin University, Changchun, Jilin 130022, China
[4]Department of Transportation Tool Application Engineering, Transportation College of Jilin University, Changchun, Jilin 130022, China

Corresponding author: Hanwu Liu (liuhanwu237@163.com)

This work was supported by the Key Research and Development and Promotion Projects in Henan Province (science and technology projects) under Grant 232102241029.

ABSTRACT This article proposes an adaptive parameter optimization energy management strategy suitable for range-extended electric vehicle (R-EEV), with the optimization objectives of improving vehicle economy, reducing emissions and extending battery life. First of all, an adaptive two-point energy management strategy (AT-PEMS) based on the auxiliary power unit (APU) optimal curve is designed, and the APU system realizes power following in the way of constant speed and variable torque. Then, the oil-electricity conversion loss rate, comprehensive exhaust emissions and battery capacity loss rate are selected as the optimization objectives, and the particle swarm optimization algorithm is applied to solve the multi-objective optimization (MOO) problem in AT-PEMS. The simulation results show that under the same solution, the three optimization objectives cannot be optimal. We evaluate the individual with the best comprehensive objective as the final optimization solution. Finally, the paper designs an adaptive parameter optimization module based on fuzzy controller. The test results show that AT-PEMS play a positive role in extending the battery life while ensuring high fuel economy and low emissions.

INDEX TERMS Range-extended electric vehicle, energy management, multi-objective optimization, adaptive fuzzy control, PSO algorithm.

I. INTRODUCTION

The rapid development of electric vehicle technology has reduced environmental pollution and the consumption of non-renewable energy to a certain extent. With the auxiliary power unit (APU) as the core power system, the range-extend electric vehicle (R-EEV) has effectively solved the problem of short drive range of battery electric vehicle, and has gradually become the main type among new energy vehicles, with good development prospects. Energy management strategy (EMS) is an important technology, which has a significant impact on the performance of R-EEV [1], [2]. The previous researches show that R-EEV can reasonably allocate the power of APU and battery to reduce the energy consumption under various working conditions and the degree of environmental pollution [3]. Therefore, EMS has a great impact on the performance of R-EEV, and a more reasonable EMS helps to improve the comprehensive performance of R-EEV [4], [5].

The associate editor coordinating the review of this manuscript and approving it for publication was Vigna K. Ramachandaramurthy.

A. LITERATURE REVIEW

The flexibility of power distribution of R-EEV vehicle system brings more complex electronic control problems. EMS can generally be divided into two categories: rule-based and optimization-based. The former can be divided into deterministic rule-based and fuzzy rule-based according to its implementation. Because of its easy implementation and high computational efficiency, it has been widely used in prac-

tice [6]. Rule-based EMS predefines relevant control rules to ensure that APU works in its efficient area. However, the development of rule-based EMS rules mainly depends on the experience of designers, and the threshold is fixed. Because the whole cycle is not optimized according to the working condition information, the rule-based EMS performance may not be optimal [7], [8], [9]. Optimization-based EMS minimizes the predefined cost function under feasible constraints, and adjusts the control variables according to the numerical calculation results. Optimization-based EMS can be further divided into global optimization control and real-time optimization control. Among them, particle swarm optimization (PSO) [10], model predictive control (MPC) [11], [12], [13], genetic algorithm (GA) [14], [15], [16], dynamic programming (DP) [17], [18], [19], pseudospectral optimal control (PSOC) [20] and minimum principle (MP) [21], [22], [23] are widely used in solving EMS MOO problems. Considering battery life, Wang et al. [24] proposed a novel EMS based on the improved deep Q-network (DQN) to reduce the driving cost of HEV, while considering the life and energy efficiency of lithium-ion batteries. Based on the DP method, the effectiveness and optimality of the proposed EMS are verified. Guo et al. [25] proposed a real-time predictive energy management strategy (PEMS) for plug-in hybrid vehicles to coordinate and control fuel economy and battery life. The results showed that the proposed PEMS has ideal performance in reducing fuel consumption and limiting battery aging. Yao et al. [26] proposed an energy management strategy based on adaptive equivalent fuel consumption minimization strategy (A-ECMS) for R-EEV, and the research results showed that it can improve battery life effectively. Zhang et al. [27] analyzed and compared the DP, Pontryagin minimum principle (PMP) and equivalent consumption minimization strategy (ECMS) of HEV considering battery aging, and finally gave their advantages and disadvantages. Based on optimization, EMS [28], [29], [30] needs to use the information of previous driving cycles and find the optimal energy allocation of various power sources of the vehicle, with the minimization of energy consumption as the control objective, which is difficult to apply in real vehicles. Therefore, EMS based on optimization is often used as a benchmark to evaluate EMS performance. In rule-based EMS, range-extended electric vehicle generally operates in two modes, namely charge depleting (CD) mode and charge sustaining (CS) mode [31]. In this paper, the CD-CS control mode is adopted, and the optimization algorithm is used to design and optimize the control parameters of the rule-based electromagnetic compatibility system from a multi-scale perspective.

The improvement of R-EEV performance not only requires to ensure higher energy efficiency but also lower emission and longer battery life as far as possible, and some previous researches on R-EEV have already concerned the MOO problem. Battery performance makes a great difference to the various performances of R-EEV, and the charging and discharging mode of battery determines the battery life [32]. Taking battery life into consideration, this paper designed an EMS for vehicles. Until now, there has also been some progress in the research of EMS in terms of battery life. Yi et al. [33] proposed a PMP global optimization algorithm for HEV that considers battery degradation and aims to optimize battery loss. Compared with fuzzy rule strategies, it effectively reduces energy consumption and delays battery loss. Anselma et al. [34] developed a battery SOH adaptive EMS using the parameters of the battery SOH function, and the results showed that the proposed method effectively improved fuel economy during battery aging. In addition, MOO problem with considering fuel consumption emissions and battery life has not been solved well. Fuel consumption, emissions and battery life should be balanced and comprehensively optimized in the real-time control system. Therefore, taking EMS as a MOO problem, this paper not only focused on minimizing energy consumption, but also considered other important performance, which made further research on EMS of R-EEV with the combination of energy efficiency, emission and battery life.

B. MOTIVATION AND INNOVATION

Compared with other control strategies, rule-based EMS is well-suited for R-EEV with the feature of high calculation efficiency. The optimal operating point of APU and the characteristic parameters of off-line optimization are the key point for EMS based on multi-objective optimization. However, the fixed parameters of EMS will not be able to match the complex changes of driving cycles to achieve the ideal comprehensive performance. Therefore, it is very important to develop an adaptive parameter optimization EMS on the basis of considering the state of the battery. This paper proposed an adaptive control strategy based on the MOO for R-EEV balancing the following three aspects: the oil-electricity conversion loss rate, the comprehensive exhaust emission and the battery capacity loss rate. The major contributions of this paper are as follows: Firstly, it proposes a general framework of MOO by BB-MOPSO which can solve the imbalanced performance problem directly and designs an AT-PEMS for APU; the MOO results can provide a reference for the establishment of rule-based control strategies. Secondly, the strategy with fixed parameters ignores the dynamic information of the battery, which makes the comprehensive indications of the strategy reduce to a certain extent. With consideration of the real-time battery SoC information, it designs an adaptive control method based on key threshold parameters of fuzzy algorithm to achieve near-optimal comprehensive performance. Thirdly, it combines offline optimization and online parameter adjustment to generate the adjustment rule base, so as to be used in real vehicles.

C. ORGANIZATION OF THIS PAPER

With consideration of SoC and current of the battery, this paper proposed a two-point energy management strategy (T-PEMS) and a MOO method to optimize energy consumption, emissions and battery life in the R-EEV. This paper is

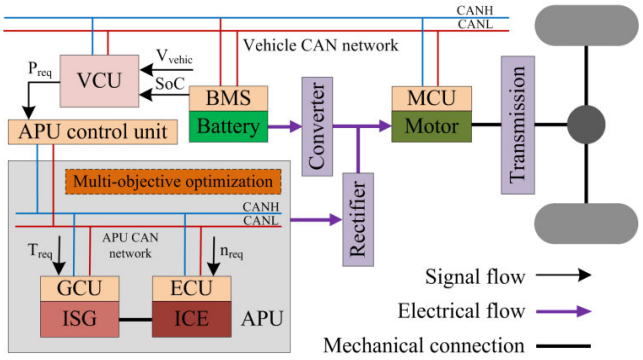

FIGURE 1. Configuration of the studied range-extended electric vehicle.

organized as follows: Section II designs the control strategy of T-PEMS and the algorithm of adaptive parameter adjustment, and introduces its principle. Section III describes the MOO problem and selects the PSO algorithm to solve the MOO problem. Section IV conducts a series of tests and figures out the pareto solution sets, and demonstrates the effectiveness and feasibility of the proposed strategy through bench tests. The last section summarizes the paper and gives the conclusion.

II. DESIGN OF ADAPTIVE TWO-POINT ENERGY MANAGEMENT STRATEGY

Rational power distribution between APU and battery is the ultimate goal of R-EEV EMS. This paper studies the control effect of the two-point energy management system of APU through the analyzation of the power distribution between APU and battery. On the basis of the T-PEMS and the operating point switching logic, it considers SoC and current of battery to contruct the parameter adjustment module based on fuzzy logic.

A. CONFIGURATION OF THE STUDIED R-EEV MODEL

This paper takes a popular configuration of R-EEV as the object, and designs relevant EMS according to its characteristics. The powertrain of this R-EEV is mainly composed of APU, battery, drive motor and transmission system, as shown in Fig. 1. The APU contains an internal combustion engine (ICE) and an integrated starter and generator (ISG). The ICE, only used to drive the ISG, can't be used to drive the wheels directly. Since the ICE speed is not coupled to the vehicle speed, it can operate continuously in the high efficiency area to achieve low fuel consumption. The battery is used to provide electrical energy for motor to compensate power and to store energy of regenerative braking.

In this paper, the CD-CS control mode is adopted. In CD mode, R-EEV is driven by pure electricity. It will switch to CS mode and APU will operate when the battery SoC reaches a lower threshold. When the required power $P_{req} < 0$, regenerative braking will be implemented, which will convert the braking energy into electric energy to the maximum and store it in the battery. The excess braking energy will be converted into friction heat by the mechanical braking system and dissipated. When $P_{req} > 0$, the APU will operate at its designed power, if the battery SoC is below its lower threshold. If the power is sufficient to meet the driving demands, most of it will be used to drive the car, the excess power will be used to charge the battery until the SoC reaches its predetermined value. If the power cannot meet the driving demands, the battery will still provide insufficient power.

B. DESIGN OF TWO-POINT ENERGY MANAGEMENT STRATEGY OF THE APU SYSTEM

As shown in Fig. 2, the T-PEMS is adopted to control APU at multiple low fuel consumption points, in which the threshold parameter is the P_{req}. APU continuously switches operating points based on the battery SoC and threshold parameters to change operating states. The operating points are determined according to the fuel consumption chart and P_{req}. The remarkable feature of this strategy is that it can effectively avoid the shortage of ICE power and the fluctuation of ICE speed and torque. This control strategy reduces the number of charge and discharge cycles, and prolongs the battery life.

The APU working mode is evenly divided into two intervals (number of constant speed operating point, $N_{csop} = 2$), and each interval corresponds to the constant speed operating point of the APU system. The maximum power in the first interval is equal to the minimum power in the second interval. Combined with the maximum power $P_{csop\_1\_max}$ and the minimum power $P_{csop\_1\_min}$ in the first interval and the power fluctuation margin coefficient ε_1, the upper and lower power limits of the APU system at the operating speed n_1 are calculated as follows, and the same applies to the upper and lower power limits of the APU system at operating speed n_2:

$$\begin{cases} P_{csop\_1\_up} = P_{csop\_1\_opt} + \frac{(P_{csop\_1\_max} - P_{csop\_1\_min})\varepsilon_1}{2} \\ P_{csop\_2\_up} = P_{csop\_2\_opt} + \frac{(P_{csop\_2\_max} - P_{csop\_2\_min})\varepsilon_2}{2} \end{cases} \tag{1}$$

$$\begin{cases} \Delta P_{1\_\varepsilon} = P_{csop\_1\_up} - P_{csop\_1\_low} \\ \Delta P_{2\_\varepsilon} = P_{csop\_2\_up} - P_{csop\_2\_low} \end{cases} \tag{2}$$

$$\begin{cases} \varepsilon_1 = \frac{\Delta P_{1\_\varepsilon}}{P_{csop\_1\_max} - P_{csop\_1\_min}} \\ \varepsilon_2 = \frac{\Delta P_{2\_\varepsilon}}{P_{csop\_2\_max} - P_{csop\_2\_min}} \end{cases} \tag{3}$$

Here, $P_{csop\_1\_up}$ and $P_{csop\_1\_low}$ are the upper and lower power limits of the APU system operating in the first interval; $P_{csop\_2\_up}$ and $P_{csop\_2\_low}$ are the upper and lower power limits of the APU system operating in the second interval; $P_{csop\_1\_opt}$ and $P_{csop\_2\_opt}$ are the power of the APU system operating at the optimal curve respectively; ε_1 and ε_2 are the power fluctuation margin coefficient respectively, which characterizes the achievable range of output power when operating at n_1 and n_2 speed. ΔP_{1_ε} and ΔP_{2_ε} are the power coverage area of the APU system operating respectively. $P_{csop\_2\_max}$ and $P_{csop\_2\_min}$ are the maximum power and minimum power of the APU system operating in the second interval.

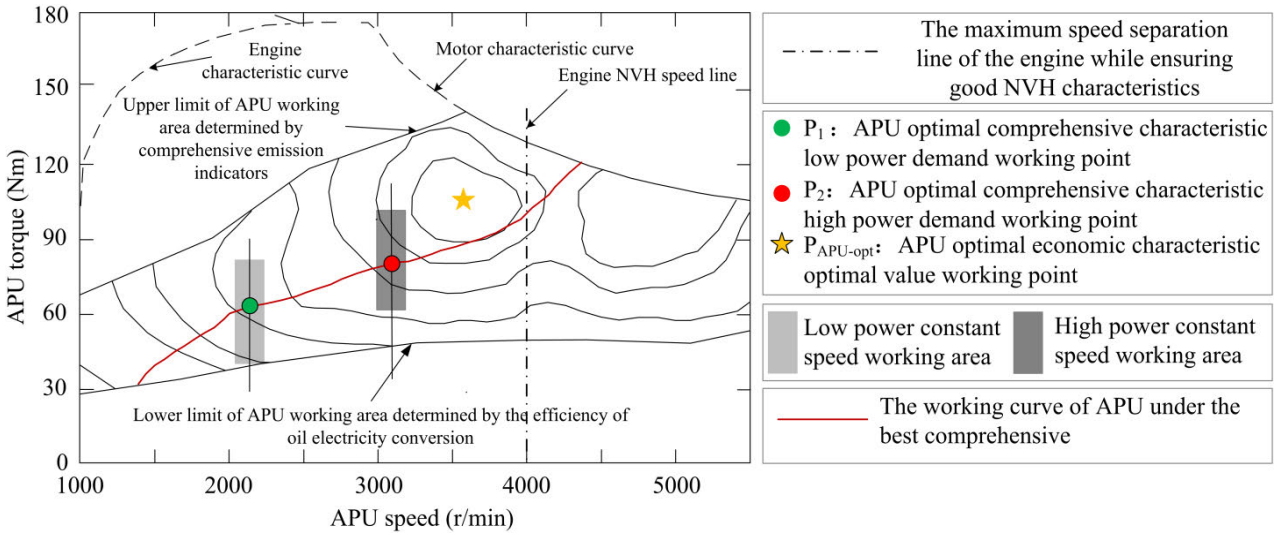

FIGURE 2. Rule-based energy management control strategy based on logic thresholds.

According to the above content, the torque at the working speed in the interval are calculated as follows:

$$\begin{cases} T_{1\_\varepsilon\_up} = \dfrac{9550P_{csop\_1\_up}}{n_1}, & T_{1\_\varepsilon\_low} = \dfrac{9550P_{csop\_1\_low}}{n_1} \\ T_{2\_\varepsilon\_up} = \dfrac{9550P_{csop\_2\_up}}{n_2}, & T_{2\_\varepsilon\_low} = \dfrac{9550P_{csop\_2\_low}}{n_2} \end{cases} \tag{4}$$

Here, $T_{1\_\varepsilon\_up}$ and $T_{1\_\varepsilon\_low}$ are the upper and lower torque limits of the APU system operating in the first interval; $T_{2\_\varepsilon\_up}$ and $T_{2\_\varepsilon\_low}$ are the upper and lower torque limits of the APU system operating in the second interval.

The switching threshold values of adjacent two operating points are set as follows:

$$\begin{cases} P_{1\_cr\_up} = P_{csop\_1\_\max}, P_{1\_cr\_low} = P_{csop\_1\_\min} \\ P_{2\_cr\_up} = P_{csop\_2\_\max}, P_{2\_cr\_low} = P_{csop\_2\_\min} \end{cases} \tag{5}$$

Here, $P_{1\_cr\_up}$ is the power threshold value of the APU system when switching from the first to the second intervals, $P_{2\_cr\_low}$ is the power threshold value of the APU system when switching from the second to the first intervals.

Therefore, the real-time target power and torque values of the APU system are calculated as follows:

$$P_{APU\_1\_act} = \begin{cases} P_{csop\_1\_low}, & P_{1\_cr\_low} \le P_{req} \le P_{csop\_1\_low} \\ P_{req}, & P_{csop\_1\_low} \le P_{req} \le P_{csop\_1\_up} \\ P_{csop\_1\_up}, & P_{csop\_1\_up} \le P_{req} \le P_{1\_cr\_up} \end{cases} \tag{6}$$

$$P_{APU\_2\_act} = \begin{cases} P_{csop\_2\_low}, & P_{2\_cr\_low} \le P_{req} \le P_{csop\_2\_low} \\ P_{req}, & P_{csop\_2\_low} \le P_{req} \le P_{csop\_2\_up} \\ P_{csop\_2\_up}, & P_{csop\_2\_up} \le P_{req} \le P_{2\_cr\_up} \end{cases} \tag{7}$$

$$T_{APU\_act} = \frac{9550P_{APU\_act}}{n_{APU\_act}} \tag{8}$$

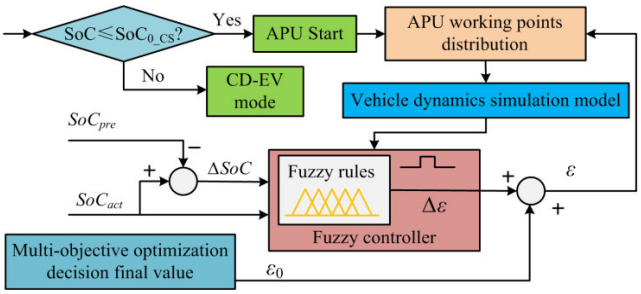

FIGURE 3. Schematic diagram of parameter adjustment of AT-PMCS.

Here, $P_{APU\_1\_act}$ and $P_{APU\_2\_act}$ are the real-time output power; n_{APU_act} is the real-time speed; T_{APU_act} is the real-time torque.

C. ADAPTIVE PARAMETER OPTIMAL ENERGY MANAGEMENT STRATEGY

The parameter fixed EMS is difficult to adapt to complex and diverse driving cycles. To reduce the adverse impact of frequent charging and discharging on the battery life, APU and battery can be effectively combined, and the energy utilization of the two can be reasonably allocated by referring to the SoC of the battery. To solve the problem that the fixed switching threshold parameters can not adapt well to the actual driving situation, this article designed a parameter adaptive optimization module based on fuzzy algorithms. In order to distinguish from the control strategy with fixed parameters mentioned earlier, the strategy with adjustable parameters is defined as AT-PMCS, and the principle of the strategy is shown in Fig. 3.

The fuzzy logic controller is used for real-time adjustment of AT-PMCS. The composition and functional implementation of the fuzzy logic controller are shown in Table 1.

TABLE 1. Composition and functional implementation principle of fuzzy logic controller.

Process	Composition	principle	Embodiment
1	Fuzzification	Convert the input deterministic quantity into a fuzzy quantity.	(1) Input deterministic quantity: the D-value between the actual SoC of the battery and the ideal SoC, ΔSoC ∈[-0.05, 0.05]; SoC∈[0.2, 1.0]. (2) Output deterministic quantity: threshold adjustment factor Δε∈[-1，1]. (3) Membership function setting: see **Fig. 4** for details.
2	Knowledge Base	Including databases and rule libraries.	The data range and rule base of parameter adaptive fuzzy control are shown in Table 1 and related descriptions in the following text.
3	Fuzzy Reasoning	Obtain the corresponding output fuzzy quantity from the input fuzzy quantity according to the control rules.	Obtain the fuzzy set of the threshold adjustment factor Δε based on the fuzzy set of ΔSoC and SoC.
4	Defuzzification	Convert the output fuzzy quantity into a definite control quantity.	Using weighted average method to solve Defuzzification.

TABLE 2. Parameter adaptive fuzzy control rules.

$\Delta\varepsilon$		ΔSoC				
		NB	*NS*	*ZO*	*PS*	*PB*
SoC	*H*	*NS*	*NS*	*ZO*	*PS*	*PS*
	M	*ZO*	*ZO*	*ZO*	*PS*	*PS*
	L	*PB*	*PM*	*PS*	*ZO*	*ZO*

The article uses the Mamdani method for fuzzy logic calculation, selecting triangles as the input and output membership functions. Set five input membership functions of ΔSoC, namely negative big (NB), negative small (NS), zero (ZO), positive small (PS), and positive big (PB). Set three input membership functions of SoC, namely high (H), medium (M), low (L). Set seven output membership functions, namely negative large (NL), negative medium (NM), negative small (NS), zero (ZO), positive small (PS), positive medium (PM), and positive large (PL).

The rule library is designed according to the following principles: when the SoC is within a higher battery efficiency operating range, it reduces $\Delta\varepsilon$ value to increase the battery's participation in operation;When the SoC is in a lower battery efficiency operating range, increase the $\Delta\varepsilon$ value to reduce the battery's participation in operation;The fuzzy rules at two operating speeds are the same, and the control rules are shown in Table 2.

It should be noted that in order to ensure control accuracy and calculation efficiency, offline calculation methods are used, and the corresponding relationship between observed values and actual values can be calculated as follows:

$$V_f = \frac{\sum_{i=1}^{n} \omega_i \cdot V_{f\_i}}{\sum_{i=1}^{n} \omega_i} \tag{9}$$

Here, V_f is the final value; n is the number of elements, ω_i is the membersh.

III. MULTI-OBJECTIVE OPTIMIZATION FOR AT-PEMS

EMS is mainly designed to reduce energy consumption, decrease exhaust emissions and increase battery life. However, the reduction of energy consumption and emissions often leads to battery use increase, which shortens battery life. In order to reasonably coordinate the three designing objectives, this section proposes an AT-PEMS based on MOO method to balance the contradiction between energy consumption, exhaust quality and battery life.

A. DESCRIPTION OF MOO PROBLEM

There are many factors that can influence the effect of EMS control, but some factors with great randomness often change greatly in reality, such as vehicle mass, road conditions, and driving habits of driver. However, the vehicle structure parameters cannot be changed during use, which makes it difficult to fully implement the MOO model algorithm. To solve this problem, the control parameters of EMS should be optimized and changed in real time.

As mentioned above, the operating point allocation rule of APU is determined by two working points (n_1 and n_2) and power range (ε_1 and ε_2). The problem described in this section will be optimized with the objective of C_{oil_ele}, E_{com}, Q_{loss} under multi-dimensional constraints, and the overall expression of the objective is as follows:

$$J_{\min}[n_1, n_2, \varepsilon_1, \varepsilon_2] = \arg \int_0^{T_{cyc}} \omega_c C_{oil\_ele} + \omega_E E_{com} + \omega_Q Q_{loss} \tag{10}$$

Here, $J_{\min}$ is the minimum value of the multi-criteria cost function of control system. n_1, n_2, ε_1 and ε_2 are a set of optimization variables that cause the objective function to obtain its minimum C_{oil_ele}, E_{com} and Q_{loss}, respectively. C_{oil_ele} is the evaluation index of oil-electricity conversion loss rate, and E_{com} is the evaluation index of comprehensive exhaust emission. Q_{loss} is the battery capacity loss rate, ω_C, ω_E and ω_Q are the weight coefficients of C_{oil_ele}, E_{com} and Q_{loss}, respectively.

B. MULTI-OBJECTIVE OPTIMIZATION MODEL

1) OIL-ELECTRIC CONVERSION LOSS RATE (C_{oil_ele})

The economic performance of APU are mainly influenced by engine efficiency and generator efficiency. Achieving the lowest energy consumption of the APU is a main goal of studying EMS. The C_{oil_ele} of APU system can be calculated according to the following:

$$C_{oil\_ele} = 1 - \frac{360 \cdot \eta_{ele}}{\eta_{oil} \cdot \rho} \tag{11}$$

Here, η_{ele} is the power generation efficiency of the generator; η_{oil} is the efficiency between the fuel and effective power of the engine; ρ is the gasoline calorific value, which is 4.6×10^7 J / kg.

2) COMPREHENSIVE EXHAUST EMISSION (E_{com})

In order to study the relationship between R-EEV exhaust emissions and APU operating conditions, this article obtains the gas emissions of CO, CH, and NO_x through engine bench tests. Based on statistical data, the APU comprehensive exhaust emission characteristic function E_{com} is defined, and the weighted expression for parameter value normalization is as follows:

$$E_{com} = \xi_{CO} E_{CO} + \xi_{CH} E_{CH} + \xi_{NOx} E_{NOx} \tag{12}$$

Here, E_{CO}, E_{CH} and E_{NOx} are the CO, CH and NO_x gas emission characteristics functions; ξ_{CO}, ξ_{CH} and ξ_{NOx} are the weight coefficients of E_{CO}, E_{CH} and E_{NOx} respectively. $[\xi_{CO}, \xi_{CH}, \xi_{Nox}]^{\mathrm{T}} = [0.4, 0.3, 0.3]^{\mathrm{T}}$ in this paper.

To avoid making the expression complex due to different measurement units, each parameter needs to be normalized before calculation, and its expression is as follows:

$$e_{w\_j} = \frac{e_{ij} - e_{j\_\min}}{e_{j\_\max} - e_{j\_\min}}, (j = 1, 2, \ldots\ldots, n) \tag{13}$$

Here, e_{w_j} is the weighted result of *i-th* emission index; e_{ij} is the result of emission index; $e_{j\_\min}$ is the minimum value of the emission index; $e_{j\_\max}$ is the maximum value of emission index.

3) BATTERY CAPACITY LOSS RATE (Q_{loss})

Due to the focus of this study is mainly on control strategies to reduce battery capacity loss, this paper calculates the battery capacity loss rate according to the model proposed in reference [35]. In this paper, the battery operating temperature is 25°, fitting parameter are taken as $B_1 * B_2 = 0.495$, $B_2 = 0.379$. Finally, Q_{loss} is obtained as follows:

$$Q_{loss} = \int_0^{T_{cyc}} 0.495 \times \frac{dI_{bat}(t)}{dt} \times \exp(0.379 \frac{I_{bat}(t)}{A_{hcell}}) \times N_{cyc} \times \mathrm{DOD} dt \tag{14}$$

Here, T_{cyc} is the total cycle time, $I_{bat}(t)$ is the battery current; DOD is the depth of charge or discharge, DOD=0.7; N_{cyc} is life cycles, A_{hcell} is the cumulative capacity of the battery.

Considering the different physical meanings and measurement units of the three objective functions: C_{oil_ele}, E_{com} and Q_{loss}, each objective function can be normalized using the following:

$$A^{(nor)} = \frac{A_p - A_p^{\min}}{A_p^{\max} - A_p^{\min}} \tag{15}$$

Here, $A^{(nor)}$ is the normalization result of the objective function, A_p is the raw data in the pareto optimal solution set, $A_p^{\max}$ and $A_p^{\min}$ are the maximum and minimum values of the raw data in the pareto optimal solution set, respectively.

$$I_{com} = \frac{1}{\omega_c C_{oil\_ele} + \omega_E E_{com} + \omega_Q Q_{loss}} \tag{16}$$

Here, I_{com} is the comprehensive performance evaluation index of the APU system that takes into account energy consumption, emissions and battery life.

According to the content of this section, the smaller the value of C_{oil_ele}, the better the economic performance of APU; the smaller the value of E_{com}, the better the quality of exhaust emissions; the smaller the value of Q_{loss}, the smaller the degree of battery aging; the higher the value of I_{com}, the better the overall performance of the system.

C. MULTI-OBJECTIVE OPTIMIZATION ALGORITHM

Particle swarm optimization (PSO) algorithm is a bionic optimization algorithm based on multiple particles. When PSO algorithm is used to solve problems, a certain number of particles are randomly generated in the feasible region of the problem space first. Then, these particles use iterative methods to continuously update their speed and position in the search space, allowing the entire population to adjust towards better fitness. In each iteration, the optimal search direction can be obtained through information sharing and mutual cooperation between individual particles, ultimately obtaining the optimal solution. The particle has three eigenvalues: position, velocity, and fitness function. They are updated by considering their own factors, individual optimality, and global optimality. The evolutionary process is shown in Fig. 5. Because the PSO algorithm has few parameters to be adjusted, does not have too many constraints, and is easy to implement, it is very suitable for solving the energy management optimization problem of R-EEV.

The speed update formula as follows:

$$v_{ij}^{(k+1)} = \omega v_{ij}^{(k+1)} + c_1 r_1 (P_{best\_ij}^{(k)} - x_{ij}^{(k)}) + c_2 r_2 (G_{best\_ij}^{(k)} - x_{ij}^{(k)}) \tag{17}$$

Here, $v_{ij}^{(k)}$ is the speed of particle i at the *j-th* dimension component in the *k-th* generation, ω is the inertia weight, c_1 and c_2 are the individual and social learning factors respectively.

The position update formula is as follows:

$$x_{ij}^{(k+1)} = x_{ij}^{(k)} + v_{ij}^{(k+1)} \tag{18}$$

Here, $x_{ij}^{(k)}$ is the position of particle i at the *j-th* dimension component in the *k-th* generation.

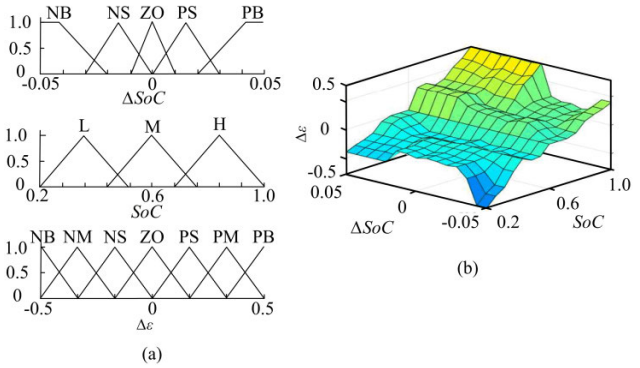

FIGURE 4. Membership function and output surface of parameter adaptive adjustment fuzzy controller.

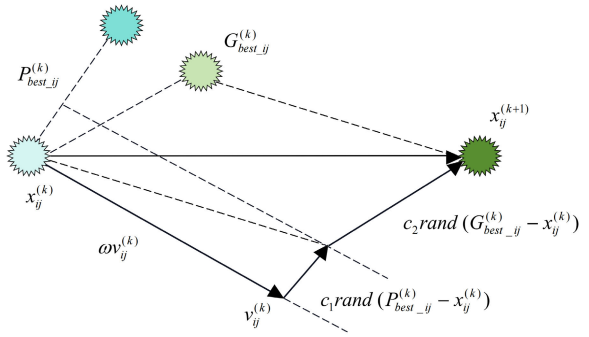

FIGURE 5. Update evolution process of traditional PSO algorithm.

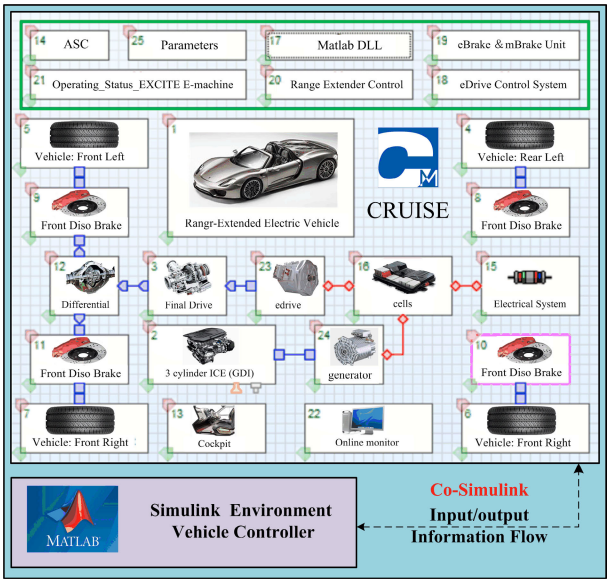

FIGURE 6. Simulation platform of the R-EEV for the MOO problem.

D. VEHICLE MODEL AND OPTIMIZATION PROCESS

The vehicle dynamic model and the proposed AT-PEMS are established in AVL/Cruise software and MATLAB/Simulink software, respectively, and the co-simulation model is shown in Fig. 6.

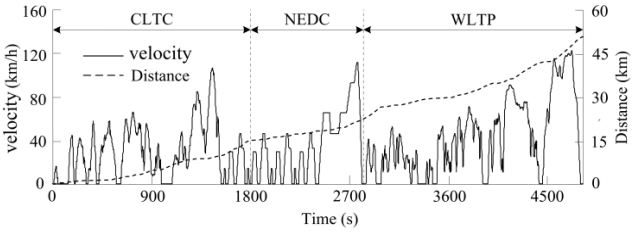

FIGURE 7. Speed and distance curves of the CCDC driving cycle.

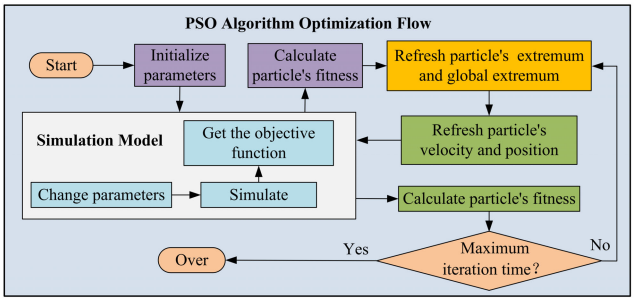

FIGURE 8. The optimization algorithm processes based on PSO.

TABLE 3. Parameters of R-EEV simulation model.

Parameter	Value
Full load weight (kg)	1700
Wheelbase (mm)	2865
Distance from front axle to centroid (mm)	1352
Distance from rear axle to centroid (mm)	1513
Centroid height (mm)	500
Drag area (m^2)	1.66
Correction coefficient of rotating mass	1.1
Mechanical efficiency	0.96
Transmission reduction ratio	4.2

Considering that the used driving cycle needs to reflect multiple types of driving cycles, this article adopts a Combined Comprehensive Driving Cycle (CCDC) composed of NEDC, CLTC, and WLTP, as shown in Fig. 7.

The fundamental parameters of the target vehicle researched are shown in Table 3.

The description of the implementation steps of optimization is shown in Fig. 8.

IV. VERIFICATION AND DISCUSSION

In this section, in order to verify that the optimal effect of the novel AT-PEMS and the proposed MOO method can achieve a better balance among the energy consumption, emissions and battery life, energy management strategies described in Section II are verified in both simulation and experimental bench.

A. INITIAL PARAMETER OPTIMIZATION RESULTS

Build and integrate the optimization model in Cruise software, and set the parameters of each module to complete the calculation. Through the data analysis window, the changes in parameter optimization results during the entire optimization

process can be observed. During the calculation process, the average value of parameters in each generation is selected to describe the changes in optimization variables during the iteration process, as shown in Fig. 9.

According to the observation of the results, all technical parameters can converge to a stable value range after approximately 60 iterations, indicating that the optimization algorithm developed in the study has good performance. However, the convergence trajectory of optimization variables during the iteration process varies, as follows:

(1) The fluctuation range of n_1 is [1100 r/min, 1750 r/min]. After approximately 30 iterations, the fluctuation range of n_1 stabilizes at [1350 r/min, 1750 r/min], and converges steadily to around 1650 r/min after 60 iterations.

(2) The fluctuation range of n_2 is [2500 r/min, 3500 r/min]. After approximately 24 iterations, the fluctuation range stabilizes at [2800 r/min, 3150 r/min], and converges to around 3000 r/min after 45 iterations.

(3) The fluctuation range of ε_1 is [0.2, 0.7]. After approximately 30 iterations, the fluctuation range stabilizes at [0.3, 0.55] and converges to around 0.42 after 50 iterations.

(4) The fluctuation range of ε_2 is [0.2, 0.8]. After approximately 30 iterations, the fluctuation range stabilizes at [0.5, 0.75] and converges to around 0.65 after 50 iterations.

The optimization results indicate that the AT-PEMS of the APU system can ensure good power performance of the R-EEV. The convergence value of the power margin value at low power operating points is relatively small, which is due to the low efficiency of the APU system in the low power operating region, resulting in the optimization results being ''compressed'' towards the low efficiency range direction; The convergence value of the power margin value at high power operating points is relatively large, which is due to the high efficiency of the APU system in the high power operating area, and the optimization results ''expand'' towards the high efficiency range. According to observation and analysis, the speed distribution in the dual operating point mode is uniform and reasonable, which can better balance the required power range during the working process.

B. COMPARISON RESULTS OF PARETO

MOO is a method to find the best solution for multiple conflicting objective functions. Any decision variable in MOO may affect the final optimization goal, and its solution set is essentially a vector optimization. When two conflicting objects appear, the plane formed by all the optimal solutions is called the ''Pareto plane''. The ultimate Pareto optimal solution is the best result among all optimal solutions, namely the ''Pareto optimal frontier''. Any solution in this result can be called optimal, and there is no reason to prove that any one of them is absolutely superior to the other solutions. This article will use the concept of Pareto advantage to evaluate the quality of solutions. For the MOO problem J (x) within the defined interval J, if there is no solution $x \in J$ and satisfies $x < x^*$, then the solution $x^* \in J$ is considered to be the Pareto optimal solution.

In the following text, this method will be used to seek a set of Pareto optimal solutions with good convergence and distribution for the MOO problem.The usual method for solving multi-objective optimization problems is to convert multi-objective problems into single objective solutions through mathematical transformation. However, in practical problems, multi-objective optimization problems often have characteristics such as nonlinearity, non-differentiability, and discontinuity, making it difficult to solve them using mathematical methods. The study of multi-objective optimization using multi-objective particle swarm optimization (heuristic algorithm) belongs to the optimal solution set acquisition strategy. The optimal solution set obtained by the algorithm is the optimal solution set of the current population, not the optimal solution of the overall problem. It can be considered as an approximate optimal solution set. Based on the definition of pareto, which is not inferior to the set composed of all other current solutions, the optimal solution set can be obtained by traversing and judging all solutions. The MOO-PSO algorithm used in this study preserves the currently found optimal solution set during each iteration, and then merges the next iteration found optimal solution set with the current optimal solution set to select the non-dominated optimal solution set again.

This section will optimize variables n_1 and n_2, ε_1 and ε_2, and obtain a set of non inferior Pareto solutions based on the PSO algorithm. The top 100 Pareto solutions among them will be used as a single objective or comprehensive objective solution set. the results are shown in Fig. 10.

Pre-adjust the APU to operate in dual point mode. Through observation and analysis, it can be concluded that when the minimum C_{oil_ele} is used as the optimization objective, the speed switching frequency is relatively small, which can balance the high demand power range with high efficiency and achieve good economic performance. Because the APU system does not achieve full power coverage, which increases the participation of batteries to some extent, the overall efficiency is not optimal. When using the minimum E_{com} as the optimization objective, if the APU parameter ε value is too small, better emission characteristics will be obtained. This is because the APU operates with a relatively small power switching frequency when ε is small, and the APU system operates more in the low emission areas. The APU output power coverage is low, and the battery participation is large, resulting in better overall efficiency. When the optimization goal is to minimize Q_{loss} and adopt a larger ε value, the APU system has high power coverage, low battery participation, and low charging and discharging power, resulting in a smaller battery capacity loss rate. When the optimization objective is I_{com}, the maximum I_{com} result is obtained when the ε value is too small. If the ε value is too large, it will cause the APU system power switching dynamic response to slow down. Therefore, it can be considered that in the mode where the ε value is relatively small, it can better balance system energy consumption, emissions, and battery capacity loss rate, thus making the comprehensive indicators better.

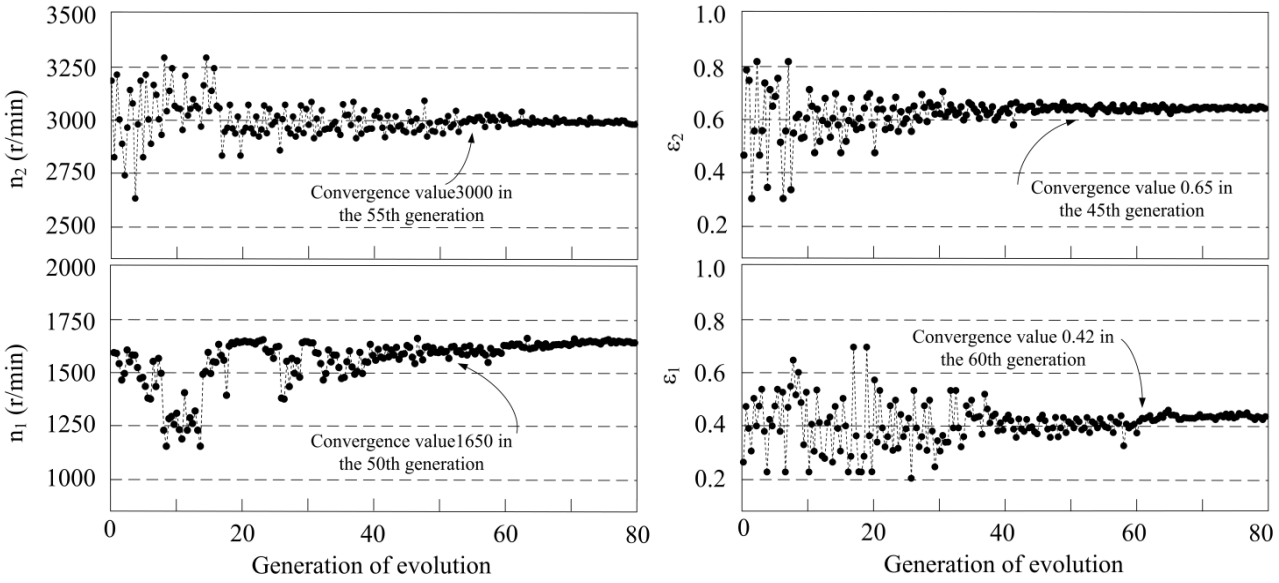

FIGURE 9. Convergence of optimization variables results during the iteration process.

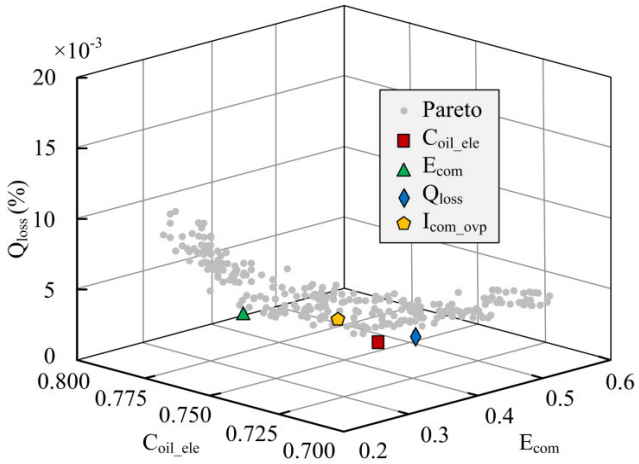

FIGURE 10. Pareto solution set of multi-objective parameter optimization of APU system in two-point operating mode.

C. COMPARISON OF THE RESULTS OF PARAMETER FIXED AND PARAMETER ADAPTIVE ADJUSTMENT

Fig. 11 shows the distribution of operating points of the APU system in two points mode of parameter fixed (T-PEMS) and parameter adaptive adjustment (AT-PEMS).

The gray hollow circle represents the position of the APU system's operating points in the MAP diagram. It can be seen that in the parameter fixed mode, the APU system operates at a fixed speed point and the optimal power curve. In the two points mode, the APU system can follow policy rules, working within the corresponding constant speed and variable torque working area to respond to demand power, the distribution of working points is uniform, the fluctuation of working speed is small, and the working points can work more near the optimal working curve. In AT-PEMS of parameter adaptive adjustment mode, some operating points have changed, with approximately 18% of the operating points shifting from low-power areas to high operating areas. At the same time, the operating points are more concentrated near the optimal operating point, which undoubtedly helps to improve the efficiency of the APU system and optimize the overall performance indicators of the system to a certain extent.

D. DISCUSSION BASED ON COMPARISON RESULTS OF STATICS ANALYSIS

Those parameter ε values are subject to considerable uncertainty or vary with their lifetimes. Comparative study against benchmark control strategy to comprehensively evaluate the proposed T-PEMS, two commonly used control strategies are introduced as comparison basics. In the following comparison and discussion, the optimization strategy is to use the work points selected based on experience as parameters before parameter optimization (BT-PEMS). After PSO optimization decision-making, the parameters will be a fixed and invariant strategy is defined as a parameter invariant strategy (T-PEMS). The strategy of adaptive optimization control is defined as an adaptive adjustment strategy (AT-PEMS). As depicted in the optimal curve region in Fig. 11, the smaller ε is, the smaller the power following coverage area is, and the APU tend to work at the optimal working point.

The charge-discharge ratio λ and APU operating point switching ratio η are introduced to discuss the test results of the three control strategies on three driving cycles (NEDC, CLTC and WLTP). λ and η are calculated as follows:

$$\lambda_{i\_C} = \frac{t_{i\_C}}{T} \tag{19}$$

$$\lambda_{i\_Dis} = \frac{t_{i\_Dis}}{T} \tag{20}$$

$$\eta_i = \frac{n_i}{N} \tag{21}$$

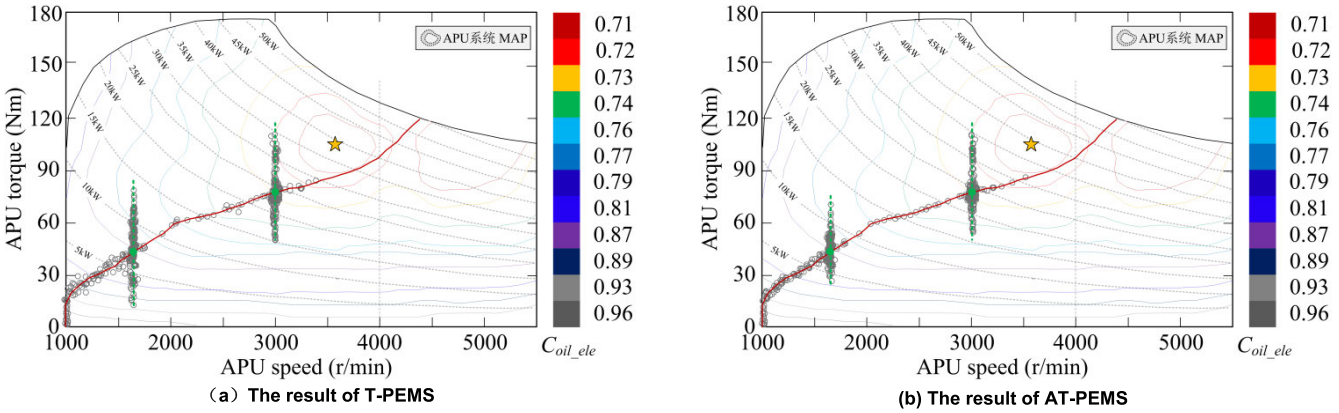

(a) The result of T-PEMS (b) The result of AT-PEMS

FIGURE 11. Distribution of operating points of APU system in two-point operating mode.

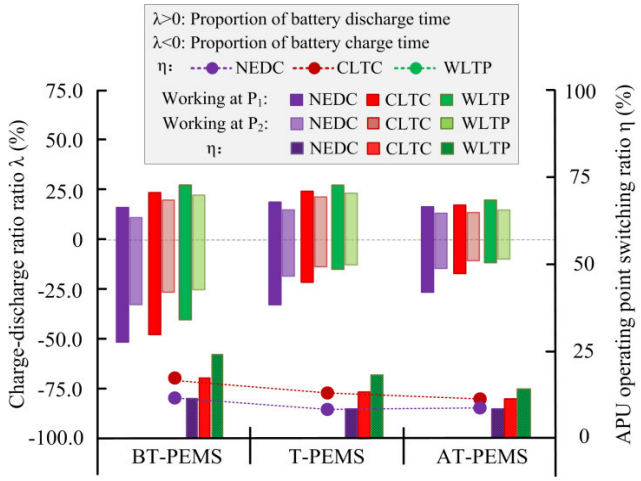

FIGURE 12. Statistical results of the control strategies on three driving cycles.

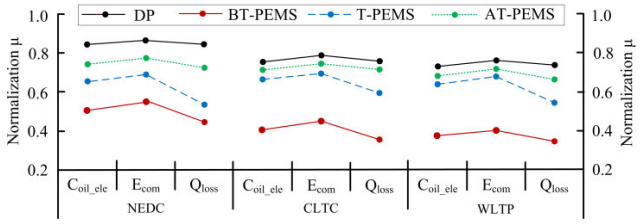

FIGURE 13. Comparison of normalized evaluation indicators: NEDC; CLTC; WLTP.

Here, λ_{i_C} and λ_{i_Dis} are the proportion of battery charging and discharging time in the i-strategy. When battery charging, $\lambda_i < 0$; when battery discharging, $\lambda_i > 0$. T is the total working time; t_{i_C} and t_{i_Dis} are the battery working charging and discharging time; η_i is the proportion of APU operating point switching times; n_i is the operating point switching times; N is the operating point times, the sampling frequency of the study is 5 Hz.

As shown in the Fig. 12, λ and η are all different and the proportion of charging on the P_1 is the largest. Further, the average working point switch frequencies (12%-24%) for APU are tolerable. In contrast, the BT-PEMS results in much more APU power transients and on-off cycles and frequent battery charging and discharging (APU works alone without battery, accounting for only about 3%). Moreover, the proposed T-PEMS urges multiple energy sources working towards more battery discharge condition, AT-PEMS can better adapt to demand power and achieve better comprehensive performance. As the working conditions become more complicated (obviously, vehicle speed/power in WLTP fluctuates greatly and irregularly than NEDC), the overall trend of statistical results between strategies is similar, the robustness of the strategies is proven. In addition to considering the results of the energy storage system, the simulation results of system fuel consumption, emission and battery life are shown in Table 4.

The developed control strategy shows good performance in energy consumption, emission and battery life. In particular, the significant reduction of battery life attenuation can greatly reduce the service cost of the whole vehicle economically. Similar to the previous study, due to the different units and scales, before comparing the performance of the three strategies on different cycles horizontally, the normalization parameters of the performance indicators are calculated as follow:

$$\mu_{ik} = \frac{I_{ik} - I_{ik}^{\min}}{I_{ik}^{\max} - I_{ik}^{\min}} \tag{22}$$

Here, μ_{ik} is the normalized index of k-th evaluation index on i-strategy; I_{ik} is the index value; $I_{ik}^{\min}$ and $I_{ik}^{\max}$ are the minimum and maximum values of the index, respectively.

DP is used as an optimal off-line baseline under the test driving cycle in this paper. And optimal control with I_{com} as the objective function. The implementation details of the DP algorithm can be found in reference [36] and [37]. Eventually, the data domain used for normalization analysis is determined, which includes the simulation results under the above strategies in NEDC, CLTC, and WLTP driving cycles, as well as and the result data under the single target based on Pareto solution set. Based on formula (22), the normalized statistical results are shown in the Fig. 13.

As shown in Fig. 13, the proposed AT-PEMS strategy has the closest performance to the DP strategy with the best

TABLE 4. Test results on CCDC.

Strategy	Fuel(L/100 km)		Emissions (g/100 km)						Battery life	
	Ge	%	CO	%	CH	%	NO_x	%	Q_{loss}	%
BT-PEMS	4.85	–	1.132	–	0.0991	–	0.087	–	12.7	–
T-PEMS	4.56	-5.98	0.976	-13.8	0.0944	-4.74	0.084	-3.45	11.7	-7.87
AT-PEMS	4.32	-10.9	0.955	-15.6	0.0916	-7.57	0.085	-2.30	10.9	-14.2

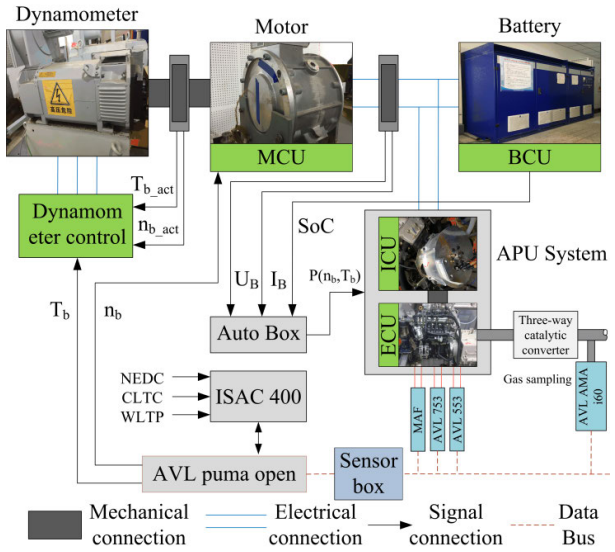

FIGURE 14. The experimental platform system structure.

TABLE 5. Vehicle components parameters of experimental platform.

Components	Parameters	Value
Engine	Maximum power / (kW)	65
	Minimum speed / (r/min)	950
	Maximum speed / (r/min)	6500
Generator	Maximum power / (kW)	60
	Maximum speed) /(r/min)	9000
Battery	Continuous discharge capacity (C)	2
	Nominal voltage/ (V)	320
	Capacity / (A·h)	25
Motor	Peak power / (kW)	75
	Maximum speed / (r/min)	9000

performance reference, and each single performance indicator in the three driving cycles is superior to the corresponding performance indicators of other strategies. By comparing the performance of each strategy in each driving cycle, it can be seen that under different cycles, the performance results of each strategy show similar performance. Among them, the AT-PEMS strategy studied in this article can achieve a better balance among the three performance goals.

E. EXPERIMENTAL TEST IMPLEMENTATION AND ITS RESULTS

As shown in the results, the different EMS significantly influence the performance. This requires further verification. The verification was completed on the AVL test bench. The experimental platform structure is shown in Fig. 14. The components parameters are shown in Table 5.

The experimental process is as follows: Firstly, vehicle parameters and preset driving cycle (WLTP) are loaded in road load simulation software. Then, the AVL system performs speed and torque closed-loop control on the motor and electric dynamometer respectively to simulate the road load of the vehicle. The real-time electric power P_{req} is calculated with the DC bus voltage and current consideration. Further then, control system collects the battery SoC and executes the T-PEMS, and outputs the engine target speed and generator target torque. Finally, APU coordinated control strategy completes the power output of the APU system. To realize the verification of the power trajectory tracking, the calculated APU power is regarded as the target power; then, experimental on three strategies proposed were implemented. The test results compares the fuel economy, exhaust emission and final battery SoC for control strategies ran over two repeated CCDC. The terminal SoC of the three control strategies are different, it is unreasonable to directly evaluate the fuel consumption value. The comparison of 100 km equivalent fuel consumption (Ge) between three control strategies after the modification of terminal SoC (the SoC corrected fuel efficiencies) are shown in Table 6.

The total consumption of the original strategy with BT-PEMS slightly increased by about 2.85% than those of the T-PEMS, and the results of the AT-PEMS are better than those of the T-PEMS by approximately 10.1%. Hence, it can be concluded that AT-PEMS is slightly better than the T-PEMS. Compared with BT-PEMS, the E_{com} of T-PEMS and AT-PEMS are reduced by about 1.2% and 1.89%, respectively. This proves that the proposed AT-PEMS can achieve higher emission quality. In contrast, the BT-PEMS emission quality is poor due to the reality that the APU operating point switches frequently. The proposed AT-PEMS will adjust the APU works on the P_{csop_1} or optimal efficiency curve to reduce the number of switching times, which is the main reason for the reduction of the total consumption.

Compared with BT-PEMS, the Q_{loss} of T-PEMS and AT-PEMS significantly are reduced by about 19.1% and 28.9%, respectively. The battery capacity of R-EEV decreases to less than 30% of the new battery state, which can be regarded as the end of the service life. In other words, the life span of the battery in the presently proposed configuration is about 1.3 times of that in conventional rule-based strategies without SoC information consideration during the whole trip. The results of the experimental are consistent with the conclusions of the simulation results. The proposed AT-PEMS is optimized to change the APU working point for reduce battery capacity loss rate. Synthetically, considering these three factors, there is obvious difference between strategies. In summary, the energy management results are confirmed to be feasible, and the results proved

TABLE 6. Test results of experimental test.

Strategy	Ge (L/100 km)	ΔGe	C_{oil_ele}	ΔC_{oil_ele}	E_{com}	ΔE_{com}	Q_{loss}	ΔQ_{loss}
BT-PEMS	4.92	–	74.6	–	0.582	–	15.2%	–
T-PEMS	4.78	-2.85%	73.3	-1.07 %	0.575	-1.20%	12.3%	-19.1%
AT-PEMS	4.42	-10.1%	73.1	-2.01%	0.571	-1.89%	10.8%	-28.9%

that the proposed T-PEMS with parameter adjust module based on MOO in the mode of taking comprehensive curve as reference, AT-PEMS could achieve a more comprehensive vehicle performance (good balance between multiple goals). Although the energy consumption could be slightly compromised, the comprehensive performance can be improvement significantly. This research and optimization method may provide a more useful reference for the design and optimization of EMS.

V. CONCLUSION

In order to effectively achieve the goals of energy conservation, emission reduction, and long service life of power batteries in R-EEV, this paper studies the system oil to electricity conversion loss rate C_{oil_ele}, comprehensive exhaust emission characteristic function E_{com}, and battery capacity loss rate Q_{loss} under different operating modes of the APU system from the perspective of multi-objective optimization. Using the PSO algorithm to solve the multi-objective optimization problems involved, the APU system's working mode/region optimization design is carried out based on the dual operating point speed value of the APU system and the power range (power fluctuation margin coefficient ε_i) corresponding to this operating point as the optimization objects, and the key parameters in the control strategy are optimized and analyzed.

After analyzing and researching the entire text, the following conclusions can be drawn: (1) The APU system designed in this study has good performance in three aspects: energy consumption, exhaust emissions, and battery capacity attenuation under N_{csop} =2 operating mode, with high I_{com} performance indicators. (2) Utilize adaptive parameter adjustment using fuzzy algorithms to adjust charging and discharging based on the battery SoC. According to the experimental results, reducing the current and frequency of charging or discharging power batteries while maintaining the same energy consumption and emission levels can effectively improve their service life. (3) Compared with the strategy without parameter optimization, the optimized strategy significantly improves energy consumption, exhaust emissions, and battery capacity degradation. Through experimental analysis, the control strategy adopted in this article is feasible and has certain promotion value in the application of R-EEV.

The research work carried out in this article mainly solves some problems of the current R-EEV energy management strategy. During the research process, intelligent energy management strategies and experimental research were conducted on the target problem. The research results can provide some reference for the theoretical research on energy management of R-EEV, and also provide a certain technical reference for the industrial production technology of R-EEV. In the subsequent research work, it is possible to further improve the prediction model of future operating conditions, integrate the deep reinforcement learning algorithm with model predictive control, and improve the performance of MPC based energy management strategy in a data-driven manner. At the same time, considering that the application of autonomous driving technology on R-EEV will lead to changes in energy management technology, future work will focus on researching how to more fully utilize various sensors on R-EEV to collect multi-dimensional information, in order to propose more intelligent energy management strategy methods and improve the overall performance of the vehicle.

REFERENCES

[1] Y. Wang, D. Lou, N. Xu, L. Fang, and P. Tan, "Energy management and emission control for range extended electric vehicles," *Energy*, vol. 236, Dec. 2021, Art. no. 121370.

[2] H. Liu, Y. Lei, Y. Fu, and X. Li, "A novel hybrid-point-line energy management strategy based on multi-objective optimization for range-extended electric vehicle," *Energy*, vol. 247, May 2022, Art. no. 123357.

[3] J. Li, X. Jin, and R. Xiong, "Multi-objective optimization study of energy management strategy and economic analysis for a range-extended electric bus," *Appl. Energy*, vol. 194, pp. 798–807, May 2017.

[4] J. Du, J. Chen, Z. Song, M. Gao, and M. Ouyang, "Design method of a power management strategy for variable battery capacities range-extended electric vehicles to improve energy efficiency and cost-effectiveness," *Energy*, vol. 121, pp. 32–42, Feb. 2017.

[5] H. Liu, Y. Lei, Y. Fu, and X. Li, "Parameter matching and optimization for power system of range-extended electric vehicle based on requirements," *Proc. Inst. Mech. Eng., D, J. Automobile Eng.*, vol. 234, no. 14, pp. 3316–3328, Dec. 2020.

[6] N. B. Halima, M. Chaieb, N. B. Hadj, R. Abdelmoula, and R. Neji, "Study of a parallel hybrid electric vehicle performance by means of rules-based control strategies," in *Proc. 17th Int. Multi-Conf. Syst., Signals Devices (SSD)*, Jul. 2020, pp. 703–708.

[7] A. Alsharif, C. W. Tan, R. Ayop, K. Y. Lau, and A. M. Dobi, "A rule-based power management strategy for vehicle-to-grid system using antlion sizing optimization," *J. Energy Storage*, vol. 41, Sep. 2021, Art. no. 102913.

[8] J. Kang, Y. Guo, and J. Liu, "Rule-based energy management strategies for a fuel cell-battery hybrid locomotive," in *Proc. IEEE 4th Conf. Energy Internet Energy Syst. Integr. (EI)*, Oct. 2020, pp. 45–50.

[9] H. Jbari, M. Haidoury, R. Askour, and B. Idris, "Rule-based energy management strategy for a pure electric vehicle," in *Proc. Int. Conf. Adv. Energy Mater. Res. (ICAEMR)*, Feb. 2021, pp. 18–25.

[10] Y. Ma and Q. Liu, "Real-time application optimization control algorithm for energy management strategy of the hybrid power system based on artificial intelligence," *Mobile Inf. Syst.*, vol. 2021, pp. 1–13, Nov. 2021.

[11] Y. Liu and J. Zhang, "A model predictive control-based energy management strategy considering electric vehicle battery thermal and cabin climate control," in *Proc. Design Automat. Conf., ASME Int. Design Eng. Tech. Conf., Comput. Inf. Eng. Conf. (ASME)*, Aug. 2020, pp. 1–11.

[12] C. Guo, D. Cao, Y. Qiao, Z. Yang, Z. Chang, D. Zhao, and Z. Hou, "Energy management strategy of extended-range electric bus based on model predictive control," *SAE Int. J. Commercial Vehicles*, vol. 14, no. 2, pp. 229–238, Feb. 2021.

[13] S. East and M. Cannon, "Energy management in plug-in hybrid electric vehicles: Convex optimization algorithms for model predictive control," *IEEE Trans. Control Syst. Technol.*, vol. 28, no. 6, pp. 2191–2203, Nov. 2020.

[14] T. Zhu, L. Wang, X. Na, T. Wu, and R. Jiang, "Research on novel fuzzy control strategy of hybrid electric vehicles based on feature selection genetic algorithm," *Sensors Mater.*, vol. 33, no. 1, pp. 301–313, May 2021.

[15] X. Lü, Y. Wu, J. Lian, Y. Zhang, C. Chen, P. Wang, and L. Meng, "Energy management of hybrid electric vehicles: A review of energy optimization of fuel cell hybrid power system based on genetic algorithm," *Energy Convers. Manage.*, vol. 205, Feb. 2020, Art. no. 112474.

[16] A. Afzal, "Optimization of thermal management in modern electric vehicle battery cells employing genetic algorithm," *J. Heat Transf., Trans. ASME*, vol. 143, Nov. 2021, Art. no. 112902.

[17] X. Xu, G. Li, and H. Zhang, "Optimal energy management system design based on dynamic programming for battery electric vehicles," in *Proc. 3rd IFAC Workshop Pn Cyber-Phys. Hum. Syst. (IFAC)*. Dec. 2020, vol. 53, no. 5, pp. 634–637.

[18] Y. Kong, N. Xu, Q. Liu, Y. Sui, and F. Yue, "A data-driven energy management method for parallel PHEVs based on action dependent heuristic dynamic programming (ADHDP) model," *Energy*, vol. 265, Feb. 2023, Art. no. 126306.

[19] N. Xu, Y. Kong, J. Yan, Y. Zhang, Y. Sui, H. Ju, H. Liu, and Z. Xu, "Global optimization energy management for multi-energy source vehicles based on 'information layer-physical layer-energy layer-dynamic programming' (IPE-DP)," *Appl. Energy*, vol. 312, Apr. 2022, Art. no. 118668.

[20] G. Yang, J. Li, and Z. Fu, "Optimization of logic threshold control strategy for electric vehicles with hybrid energy storage system by pseudo-spectral method," in *Proc. Appl. Energy Symp. Forum, Conf. (CUE)*, Jun. 2018, vol. 152, no. 5, pp. 508–513.

[21] Y. Wang, Z. Wu, Y. Chen, A. Xia, C. Guo, and Z. Tang, "Research on energy optimization control strategy of the hybrid electric vehicle based on Pontryagin's minimum principle," *Comput. Electr. Eng.*, vol. 72, pp. 203–213, Nov. 2018.

[22] S. Xie, X. Hu, Z. Xin, and J. Brighton, "Pontryagin's minimum principle based model predictive control of energy management for a plug-in hybrid electric bus," *Appl. Energy*, vol. 236, pp. 893–905, Feb. 2019.

[23] K. Song, X. Wang, F. Li, M. Sorrentino, and B. Zheng, "Pontryagin's minimum principle-based real-time energy management strategy for fuel cell hybrid electric vehicle considering both fuel economy and power source durability," *Energy*, vol. 205, Aug. 2020, Art. no. 118064.

[24] H. Wang, H. He, Y. Bai, and H. Yue, "Parameterized deep Q-network based energy management with balanced energy economy and battery life for hybrid electric vehicles," *Appl. Energy*, vol. 320, Aug. 2022, Art. no. 119270.

[25] N. Guo, X. Zhang, Y. Zou, L. Guo, and G. Du, "Real-time predictive energy management of plug-in hybrid electric vehicles for coordination of fuel economy and battery degradation," *Energy*, vol. 214, Jan. 2021, Art. no. 119070.

[26] D. Yao, X. Lu, X. Chao, Y. Zhang, J. Shen, F. Zeng, Z. Zhang, and F. Wu, "Adaptive equivalent fuel consumption minimization based energy management strategy for extended-range electric vehicle," *Sustainability*, vol. 15, no. 5, p. 4607, Mar. 2023.

[27] F. Zhang, L. Xiao, S. Coskun, H. Pang, S. Xie, K. Liu, and Y. Cui, "Comparative study of energy management in parallel hybrid electric vehicles considering battery ageing," *Energy*, vol. 264, Feb. 2023, Art. no. 123219.

[28] Z. Chen, Y. Liu, M. Ye, Y. Zhang, Z. Chen, and G. Li, "A survey on key techniques and development perspectives of equivalent consumption minimisation strategy for hybrid electric vehicles," *Renew. Sustain. Energy Rev.*, vol. 151, Nov. 2021, Art. no. 111607.

[29] T. Zeng, C. Zhang, Y. Zhang, C. Deng, D. Hao, Z. Zhu, H. Ran, and D. Cao, "Optimization-oriented adaptive equivalent consumption minimization strategy based on short-term demand power prediction for fuel cell hybrid vehicle," *Energy*, vol. 227, Jul. 2021, Art. no. 120305.

[30] H. Dong, Z. Zhao, J. Fu, J. Liu, J. Li, K. Liang, and Q. Zhou, "Experiment and simulation investigation on energy management of a gasoline vehicle and hybrid turbocharger optimization based on equivalent consumption minimization strategy," *Energy Convers. Manage.*, vol. 226, Dec. 2020, Art. no. 113518.

[31] J. M. Pi, Y. S. Bak, Y. K. You, D. H. Park, and H. S. Kim, "Development of route information based driving control algorithm for a range-extended electric vehicle," *Int. J. Automot. Technol.*, vol. 17, no. 6, pp. 1101–1111, Dec. 2016.

[32] X. Ma, Y. Zhang, C. Yin, and S. Yuan, "Multi-objective optimization considering battery degradation for a multi-mode power-split electric vehicle," *Energies*, vol. 10, no. 7, p. 975, Jul. 2017.

[33] F. Yi, D. Lu, X. Wang, C. Pan, Y. Tao, J. Zhou, and C. Zhao, "Energy management strategy for hybrid energy storage electric vehicles based on Pontryagin's minimum principle considering battery degradation," *Sustainability*, vol. 14, no. 3, p. 1214, Jan. 2022.

[34] P. Anselma, P. Kollmeyer, and A. Emadi, "Battery state-of-health adaptive energy management of hybrid electric vehicles," in *Proc. IEEE/AIAA Transp. Electrific. Conf., Conf. (ITEC+EATS)*, Jun. 2022, pp. 1035–1040.

[35] H. Liu, Y. Lei, Y. Fu, and X. Li, "An optimal slip ratio-based revised regenerative braking control strategy of range-extended electric vehicle," *Energies*, vol. 13, no. 6, p. 1526, Mar. 2020.

[36] X. Tang, L. Chu, N. Xu, D. Zhao, and Z. Xu, "Energy management of planetary gear hybrid electric vehicle based on improved dynamic programming," in *Proc. Int. Conf. Neural Inf. Process. (ICONIP)*, vol. 10639. Cham, Switzerland: Springer, Jan. 2017, pp. 130–138.

[37] Z. Wei, J. Xu, and D. Halim, "HEV power management control strategy for urban driving," *Appl. Energy*, vol. 194, pp. 705–714, May 2017.

CHENG CHANG received the bachelor's degree in vehicle engineering from the Henan University of Science and Technology, in 2010, and the Ph.D. degree in vehicle engineering from Jilin University, in 2017.

He is currently with the School of Vehicle and Traffic Engineering, Henan Institute of Technology. His current research interests include optimization design of electric vehicle structure, control algorithm for electric vehicles, and optimization of eddy current retarder control.

ZIKAI FAN received the B.S. degree in vehicle engineering from Yantai University, Yantai, China, in 2021. He is currently pursuing the M.S. degree in vehicle engineering with Jilin University, Changchun, China.

His research interest includes energy management strategies for hybrid electric vehicles.

ZHIHUI WANG is currently pursuing the bachelor's degree in vehicle engineering with the Henan Institute of Technology.

Her research interest includes modeling and simulation experiments for new energy electric vehicles.

HANWU LIU received the Ph.D. degree in vehicle engineering from the School of Automotive Engineering, Jilin University.

He is currently with the Transportation College of Jilin University. His research interests include the optimization of powertrain parameters, energy management strategy, and online intelligent control strategy for PHEV.